Fatty acids associated with the frustules of diatoms and their fate during degradation -- A case study in Thalassiosira weissflogii — Source link ⤢

Maxime Suroy, Brivaëla Moriceau, Julia Boutorh, Madeleine Goutx

Institutions: Aix-Marseille University, IFREMER

Related papers:

- Tinted windows: The presence of the UV absorbing compounds called mycosporine-like amino acids embedded in the frustules of marine diatoms

- Analysis of natural diatom communities reveals novel insights into the diversity of long chain polyamine (LCPA) structures involved in silica precipitation

- Structural identification of long-chain polyamines associated with diatom biosilica in a Southern Ocean sediment core

- Degradation and dissolution of zooplanktonic organic matter and lipids in early diagenesis

- Production and export of particulate fatty acids, carbohydrates and combined amino acids in the euphotic zone

Fatty acids associated with the frustules of diatoms and their fate during degradation – A case study in Thalassiosira weissflogii

Maxime Suroy, Brivaëla Moriceau, Julia Boutorh, Madeleine Goutx

1   Fatty acids associated with the frustule of diatoms and their fate during

2   degradation – a case study in *Thalassiosira weissflogii*.

3   Maxime Suroy[1], Brivaëla Moriceau[2], Boutorh Julia[2], Madeleine Goutx[1].

4   [1]Aix-Marseille Université, Université du Sud Toulon-Var, CNRS/INSU, IRD,

5   Mediterranean Institute of Oceanography (MIO), UM 110, 13288, Marseille, Cedex 09,

6   France.

7   [2]Université de Brest, Institut Universitaire Européen de la Mer (IUEM), CNRS,

8   Laboratoire des Sciences de l'Environnement Marin, UMR 6539

9   CNRS/UBO/IFREMER/IRD, 29280 Plouzané, France.

10   Corresponding author: Suroy, Maxime:Maxime.suroy@univ-amu.fr. Tel. +0033 491829050

11

12   **Abstract*:***

13   Diatoms are major actors in the export of organic carbon out of the euphotic zone. Yet,

14   the processes linking biogenic silica and carbon sedimentation fluxes to deep oceanic layers

15   remain unclear. Analysing organic fractions in biominerals is challenging because efficient

16   cleaning often led to structural alteration of organic molecules. Hence, although lipids are

17   widely used as biogeochemical markers in ocean flux study, few studies have dealt with the

18   lipids that are associated with frustules. In the present study, a protocol was set up to extract

19   and quantify the fatty acids associated to the frustule of the diatom species *Thalassiosira*

20   *weissflogii*. The protocol involves solvent extraction of diatom external lipids, followed by

21   clean frustule dissolution by 4% NaOH during 1h at 95°C and subsequent solvent re-

22   extraction of frustule-associated lipids. Results confirmed that this protocol was efficient first,

23   to isolate the frustule from the rest of the cellular organic carbon and second to extract and

24   quantify fatty acids (FA) associated to frustules of this species. FA composition of the

25   frustules was significantly different from that of the whole cells consisting primarily of 14:0,

26   16:0 and 18:0 FA, as well as a smaller portion of 16:1 and 18:1 unsaturated FA. Frustule-

27   associated FA constituted 7 % of the total FA and 1.8 % of the total POC. The 30 days *T.*

28   *weissflogii* degradation/dissolution experiment suggested that frustule FA 14:0 and 16:0 were

29   mainly associated with the $bSiO_2$ phase dissolving slowly as no degradation of this pool was

30   measured despite 78 % frustule dissolution. At the end of the degradation experiment, this

31   pool constituted 5.8 % of the remaining total POC suggesting an effective protection by the

32   frustule through strong interaction with the organic matrix which is consistent with the

33   correlation observed at depth between Si and POC sedimentation fluxes.

34

35   Keywords: Frustule, Diatoms, Organic Carbon, Lipids, Carbon Export

36

2

1. Introduction

Diatoms are characterised by a silicified cell wall, commonly known as the frustule. This frustule partially consists of amorphous silica that forms mineral structures by precipitation of orthosilicic acid (Martin-Jézéquel et al., 2000). Such a structure presents great evolutionary advantages to cells, such as turgor resistance and protection against predation (Raven and Waite, 2004 and reference therein), or optical properties (Kucki, 2009), partially explaining the success of diatoms and the presumed number of diatom species (more than 200 000, Mann and Droop, 1996). This success is illustrated by diatom's predominant role in primary production in the ocean (Falkowski et al., 1998) but also in the export of organic matter (OM) to the ocean depths (Nelson et al., 1995; Volk and Hoffert, 1985). Diatom frustule-bound organic compounds are diverse. The formation of the frustule starts within silicon deposition vesicles and requires a peculiar association between organic compounds and silicon (Hildebrand, 2008). Many studies have demonstrated the role of proteins and polyamines during the precipitation of silica in diatoms (Brunner et al., 2009). The presence of sugars closely associated with frustule is also confirmed in recent studies, but their role in the biomineralisation process remains unclear (Chiovitti et al., 2005; Tesson and Hildebrand, 2013). In contrast, because they are not assumed to be functionally critical to the formation of the biogenic silica, little is known about the potential association of lipids in frustules.

Diatoms (Fileman et al., 1998) and frustule-bound organic compounds (Bridoux and Ingalls, 2010; Bridoux et al., 2012; Hedges et al., 2001; Ingalls et al., 2010) provide organic matter to the sediment. Compilation of deep sedimentation fluxes of POC and minerals (Armstrong et al., 2002; Buesseler, 1998; De La Rocha and Passow, 2007) show correlations between those fluxes. More specifically, deep sedimentation fluxes of particulate organic carbon (POC) and biogenic silica ($bSiO_2$) are also correlated when expressed basin by basin (Ragueneau et al., 2006). Using an independent data base, Ragueneau and co-workers (2002)

3

62 showed that the evolution of the Si/C in all areas of the ocean can be predicted using an

63 empirical relationship. In other words, the sinking of $bSiO_2$ and POC are linked in such a

64 manner that knowing Si/C in the surface layer, one can theoretically extrapolate the flux of

65 POC from the flux of $bSiO_2$. But what processes could explain such a link between the

66 preserved fraction of organic matter and the $bSiO_2$?

67 The preservation of a fraction of organic matter during the sedimentation through the

68 water column to the sediment depends on the balance between sinking and degradation

69 processes. Biominerals in general and $bSiO_2$ in particular could impact both processes. As

70 suggested by the ballast ratio hypothesis (Armstrong et al., 2009, 2002; Klaas and Archer,

71 2002), the sinking of organic matter ballasted by dense biominerals be it as shells or once

72 incorporated to the same large particles like aggregates or fecal pellets (Thornton, 2002;

73 Turner, 2002) should be faster than the sinking of non-ballasted organic matter. Moreover

74 $bSiO_2$ may also slow down the degradation as some studies hypothesized that the diatom

75 frustule surrounding the cellular organic matter could protect the internal pool against

76 bacterial degradation (Goutx et al., 2007; Moriceau et al., 2009). But these studies were

77 undertaken on living diatoms and this hypothesis is not confirmed by degradation studies

78 made on dead diatoms (Soler et al., 2010).

79 Other studies have evidenced the presence of another organic pool intimately linked to

80 the frustule that could potentially explain the correlation between organic carbon and $bSiO_2$.

81 This fraction of organic matter preserved at great depths is proportional to the flux of

82 biominerals (Armstrong et al., 2009, 2002; François et al., 2002; Klaas and Archer, 2002;

83 Ragueneau et al., 2006, 2002). In our study, we hypothesized that the preserved organic

84 matter can be partially formed by the pool of lipids associated to or embedded in the silica

85 matrix.

86   The presence of an organic coating has been so far mainly deduced from $bSiO_2$

87   dissolution experiments on whole versus cleaned frustule (Bidle and Azam, 1999; Kamatani

88   and Riley, 1979; Patrick and Holding, 1985). From the experimental results described in the

89   study by Bidle and Azam (1999), it seems that this pool is removed by bacteria within hours

90   or few days after the death of diatoms. Only few diatoms can reach the sediment with an

91   intact organic coating as shown by a minimum of 50 % dissolution of the $bSiO_2$ observed in

92   most oceanic sites. The frustule-embedded OM is more difficult to assess as the chemical

93   reagents known to dissolve the silica (NaOH, Na_2CO_3 and HF) generally react with the

94   targeted polymer organic compounds. The inclusion of proteins in the silica matrix and their

95   implication in silicification have been well-investigated (Hildebrand, 2003; Hildebrand et al.,

96   2009; Kröger et al., 2002, 1999, 1997, 1994). The presence of other molecules less directly

97   involved on silicification processes, such as lipids or sugars, has been much less studied.

98   Kates and Volcani (1968) described the lipid composition of the cell wall for the first

99   time after breaking and washing the cells. To our knowledge, this study remains the only one

100   dealing at the molecular level with lipids associated to diatom frustules. Recent works studied

101   this organosilicon structure and noted the importance of lipid-like compounds embedded in

102   the frustule of diatoms using spectroscopic methods (Soler et al., 2010; Tesson et al., 2008).

103   These global methods that avoid dissolution procedures and the potential denaturation of most

104   organic molecules, confirm the presence of OM associated with the frustule but did not reveal

105   details about the structure and amounts of the classes of compounds detected.

106   In the present work, our approach combined the procedures of Ragueneau and Tréguer

107   (1994) and Chiovitti et al. (2005) and enabled the complete dissolution of the frustules and the

108   study of released FA. The protocol was developed on the diatom *Thalassiosira weissflogii* and

109   a 30-day dissolution/degradation experiment was carried out first to validate our protocol and

110   second to understand the fate of frustule-associated lipids during biodegradation.

5

2. Material and Methods

2.1. Culture conditions and sampling

The strain *Thalassiosira weissflogii* (CCMP n°1049) was provided by the National Centre for Marine Algae and Microbiota. Three cultures (A, B and C cultures) were grown in f/2 medium under a 14/10 h light/dark cycle at 18 °C in 2 l glass flasks (Guillard and Ryther, 1962) in sterile conditions. Culture C was grown in another growth chamber under similar growth conditions (temperature, light intensity and cycles). Differences in the carbon content of cultured cells were observed (15.6 ± 0.2, 15.6 ± 0.1 and 10.9 ± 0.1 pmol.cell^{-1} in cultures A, B and C, respectively). The cell concentration was determined by flow cytometry (FACS Calibur, BD biosciences®).

Samples were collected as soon as cultures reached the stationary phase ($\sim 10^5$ cell.ml^{-1} and 15 days of growth). Triplicate of 10 ml of culture were sampled in cultures B and C for the 'whole cells' analysis and filtered on pre-combusted GF/F filters (0.7-µm mesh size) as generally done in other studies (Table 1). Lipids from whole cells were extracted according to the Bligh and Dyer protocol (1959) and thus do not include the frustule-associated fraction. Culture A was not sampled for lipid composition analysis in whole cells. The carbon content of cells in batch A was similar to that of cells in batch B, suggesting composition similarity between A and B cultures. Except the 20:5(n-3) FA (see Fig. 4 below), this latter assumption was supported by the low SD of average percentages of individual FA in total FA, derived from the analysis of FA in triplicate samples from both B and C cultures. To obtain the 'pellet' samples, triplicates of 50 ml of the three cultures were centrifuged at 5400 *g* (20 min).

2.2. Frustule isolation

Pellet samples were resuspended in 40 ml milli*Q* water and were hot-sonicated at 70 °C for 5 min to fragment the cells (Fig. 1). Tubes were subsequently centrifuged at 5400 *g* for 40 min at 4 °C. The supernatants were removed, and this step was repeated once at lower

6

136 centrifugation speed (3800 g for 20 min) to eliminate any non-frustule material. After

137 removing the supernatant, the pellets were again resuspended in 40 ml milli$Q$ water and

138 centrifuged at 3200 g for 20 min. This treatment cleared the frustules from most cell content.

139 However, fluorescence of chlorophyll molecules was noticeable on flow cytometer analysis of

140 the washed pellets indicating external organic material still present on frustule fragments

141 (Fig.2).

142   In a second step, this external organic material probably more intimately linked to the

143 frustules than the previous cell content, was separated from fragmented frustules using a

144 modified protocol of Bligh and Dyer. Briefly, the washed pellets were transferred to glass

145 tubes. A monophasic mixture of dichloromethane/methanol/1M salt water (1/2/0.8, v/v/v) (9.5

146 ml) was added for the lipid extraction. After the addition of an internal standard

147 (nonadecanoic acid methyl ester, Me19:0, Sigma Aldrich®) and sonication (10 min), tube

148 contents were transferred to separatory funnels. Tubes were rinsed with 9.5 ml of the

149 monophasic mixture. The separatory funnel contents were made biphasic by adding 5 ml

150 dichloromethane (DCM) and 5 ml milli$Q$ water. After vigorous shaking and settling, the

151 organic phases were collected, and the aqueous phases were re-extracted with 10 ml DCM.

152 The organic phases were combined and concentrated under a gentle flux of nitrogen. The lipid

153 extracts such obtained from the pellets of isolated frustules constituted our lipid 'external'

154 fractions.

155 **2.3.   Extraction of frustule-associated lipids**

156   Frustules cleaned from their 'external' fraction were visualised by scanning electronic

157 microscopy during the cleaning procedure to check for their integrity and the absence of

158 'external' organic matter at the end of this step. Frustule fragments formed a white layer at the

159 basis of the aqueous phase (methanol/water mixture) remaining in the separatory funnel after

160 the Bligh and Dyer extraction (Fig. 1). Scanning electron microscopy analysis of this white

7

161   layer samples showed an amalgam of clean silica frustules (Fig. 3). Hydrophilic compounds

162   that may be present in the aqueous phase were not analysed further. The white layer and the

163   top aqueous phase were transferred into glass bottle in which sodium hydroxide (1 mol.l^{-1}

164   final concentration) was added. These bottles were later transferred to a water bath at 95 °C

165   for 1 h to promote the entire dissolution of frustules. The basic reactant not only dissolves the

166   silica matrix but can cleave covalent associations between FA and polymers. After a rapid

167   cooling on ice, the bottle contents were acidified using HCl and re-extracted in a liquid-liquid

168   phase using 50 ml DCM (the aqueous phase was approximately 70 ml). This last extraction

169   step was repeated three times to ensure the complete extraction of the remaining lipids in the

170   aqueous phase. Extracts thus obtained were called the 'frustule-associated' fractions. The

171   internal standard (Me19:0) was not added before dissolved frustule extraction in order to

172   control the absence of contamination in the 'frustule-associated' extract from the 'external'

173   fraction. Consequently, the same extraction recovery was used for the quantification of both

174   'external' and 'frustule-associated' lipids.

175   **2.4. Biodegradation experiment**

176   For the degradation experiment, the *T. weissflogii* strain was supplied and grown in a

177   large volume culture by the Experimental Station of Argenton (Ifremer, France). Cells were

178   pelleted and killed by freezing at -20 °C for 4 days. Pellets were resuspended in a Nalgene®

179   flask filled with 10 l of 0.7-µm filtered seawater from Brest Bay (France). The 0.7-µm filtered

180   water contained the natural prokaryotic community required to degrade and utilize the algal

181   material as growth substrate. The flask was incubated on an orbital shaker table at 70 rpm in

182   the dark at 18 °C. The degradation experiment lasted 30 days. Samples (50 ml) were collected

183   from the flask every 6 days, in duplicate or triplicate, and subjected to centrifugation for

184   frustule isolation and lipid extraction as described in the previous section. Briefly, cells were

185   sonicated, pelleted to remove medium and extracted according to Bligh and Dyer for analysis

8

186 of external FA composition. Cleaned frustules were submitted to NaOH dissolution and re-

187 extracted for analysis of frustule-associated FA fraction.

2.5. Bulk parameters: $bSiO_2$, POC and prokaryotic concentrations

189       $bSiO_2$ and POC concentrations were followed during the whole degradation

190 experiment by filtering 10 ml of the batch content on polycarbonate (0.4-µm mesh size) and

191 GF/F (0.7-µm mesh size) filters, respectively.

192       $bSiO_2$ concentrations were measured using a variation of the method of Ragueneau

193 and Tréguer (1994) described in Moriceau et al. (2009). Filters were digested in 20 mL of 0.2

194 M NaOH for 3 hours at 95°C and stirred regularly to ensure the dissolution of all $bSiO_2$. As

195 no lithogenic silica was present in the diatom culture, only one longer digestion step was

196 done. The solution was then acidified with 5mL of HCl 1M, centrifuged to remove solids and

197 analysed for silicic acid concentrations (dSi). dSi was measured using the molybdate blue

198 spectrophotometric method of Mullin and Riley (1955), as adapted by Tréguer and Le Corre,

199 (1975) and modified by Gordon et al. (1993) for use in segmented flow colorimetry. We used

200 a Bran and Luebbe Technicon Autoanalyser (<1% precision).POC filters were desiccated

201 overnight in an oven at 50 °C, and POC was quantified by using a Carlo Erba NA 2100 CN

202 analyser coupled to a Finnigan Delta S mass spectrometer.

203   Prokaryotes were counted over time in 10 ml samples to assess their growth. Free and

204 attached prokaryotes were separated by filtration (3-µm mesh size) and counted on black 0.2-

205 µm filters after staining with DAPI (4',6-diamidino-2-phenylindole).

206   Prokaryotic carbon in degradation flask samples was calculated by using conversion

207 factors (20 and 50 x 10^{-15} molC.cell^{-1} for free and attached prokaryotes, respectively)

208 according to Turley and Mackie (1994) for the north-eastern Atlantic Ocean.

9

2.6. Lipid analysis

2.6.1. Derivatisation and purification.

Lipid extracts were trans-esterified using BF_3-Methanol and toluene for 1 h at 70 °C. Fatty acid methyl esters (FAME) were extracted from the mixture with 3 x 2 ml of Hexane/Ethyl Ether (98/2, v/v) and evaporated to dryness under nitrogen. FAME were purified onto a bond elute microcolumn with a mix of Hexane-Ethylacetate (99/1, v/v). Columns were conditioned with 9 ml Hexane-Ethyl Acetate (99/1, v/v) followed by 3 ml Hexane. Columns were rinsed with 1.4 ml Hexane (to remove hydrocarbons), and FAMEs were eluted by 1.6 ml Hexane-Ethyl Acetate (99/1, v/v).

Extracts from the degradation experiment were first saponified (KOH 1 mol.l^{-1} for 1 h at 70 °C) and were silylated using a N,O-bis(trimethysilyl)trifluoroacetamide (BSTFA)-pyridine mixture according to Rontani et al. (2011). Briefly, after saponification, BSTFA and pyridine were added to the dried lipid extract (1/2, v/v). Tubes were placed at 50 °C for 1 h, and then their contents were dried under a gentle stream of nitrogen and resuspended in ethyl acetate and BSTFA. This reaction transforms OH-containing molecules to their trimethylsilyl (TMS) derivatives. Injections of trimethylsilyl ether (TMSE) were made in the 12 hrs following derivatisation due to their unstable nature. This method allowed us to analyse FA, sterols and phytol simultaneously in their TMS ether forms. Indeed, the phytil side chain of chlorophyll is released during saponification (phytol) and transformed to its TMS derivative. Sterols are also present in diatoms, primarily in a free form (*i.e.*, non-esterified, Volkman and Hallegraeff, 1988). Four sterols (Volkman and Hallegraeff, 1988) were identified, but we combined them in this study. Sterols were quantified by reference to a calibration curve of a cholesterol standard. The quantification of phytol was semi-quantitative using a calibration curve of TMS20:0.

233   The impact on PUFA of the step involving heating the silica/organic matter complex

234   was tested. The percentage recoveries of arachidonic acid (20:4(n-6)) after incubation for one

235   hour both at 40 °C and 70 °C were in the range of the RSD. Other authors also reported

236   saponification of lipid extracts at 100 °C without noticeable effect on poly-unsaturated FA

237   quantification (Chen et al., 2011; Goutx et al., 2007).

238   2.6.2. **GC/MS analysis.**

239   FAME and TMSE were analysed by gas chromatography/mass spectrometer (GC/MS)

240   (TraceISQ, ThermoElectron) at an ionization energy of 70 eV for *m/z* range of 50-400 for

241   FAME and 50-600 for TMSE, using hydrogen as carrier gas at a flow rate of 1.2 ml.min^{-1}.

242   The injector (used in splitless mode) and detector temperatures were 250 and 320 °C

243   respectively. For FAME analysis, the initial column temperature was held for 2 min at 70 °C

244   then ramped at 12 °C.min^{-1} (ramp 1) to 140 °C, and then at 5 °C.min^{-1} (ramp 2) to 200 °C,

245   which was held for 5 min, then finally ramped at 12 °C.min^{-1} (ramp 3) to 275 °C and held for

246   10 min. FA, sterols and phytol from the degradation experiment were analysed in their TMS

247   forms using the same conditions as FAME analysis on the same GC/MS. The ramp

248   temperature only was modified as follow: the initial temperature was set at 70 °C and

249   successively increased to 130 °C at 20 °C.min^{-1}, then to 250 °C at 5 °C.min^{-1} and finally at 3

250   °C.min^{-1} to 300 °C, held for 40 min. The source temperature was set at 200 °C. FAME and

251   TMSE were identified by comparison with retention time and mass spectra of commercial

252   standards (provided by Sigma Aldrich®) and quantified by reference to calibration curves.

253   The positions of the double bounds were all identified with the exception of that of 16:1, 16:2

254   and 24:1 for which we did not run standards. All determination coefficients were up to 0.99.

255   Tricosanoic acid methyl ester standard (Me23:0) was introduced prior to injection to check

256   analytical variability. The mean analytical recovery, taking into account all preparative steps

257   except dissolution, was in the range of the Relative Standard Deviation (4 to 9 % for peak

11

258   areas and from 0.04 to 0.11 % for the retention time) and was approximately 83 %. As we did

259   not add any standard to the frustule-bound fraction, internal standard (19:0 in its trimethylsilyl

260   or methyl form) was used to check whether any cellular material (that contained the internal

261   standard) may have contaminated the 'frustule-bound' fraction. All concentration values were

262   blank and recovery corrected.

263   **2.7. Flow cytometry.**

264   Samples were analysed using the FACSCalibur (BD Biosciences[®]) of the PRECYM

265   flow cytometry platform (http://precym.com.univ-mrs.fr) equipped with a blue (488 nm) air-

266   cooled argon laser and a red (634 nm) diode laser. Data were collected using the CellQuest

267   software (BD Biosciences[®]). The analysis was performed *a posteriori* using SUMMIT v4.3

268   software (Beckman Coulter). *T. weissflogii* cells were optically resolved based on their

269   intensities in light scatter and red fluorescence (chlorophyll *a* related). TruCount beads (BD

270   Biosciences[®]) and 2-µm beads (Fluoresbrite YG, Polyscience[®]) were added to the samples as

271   an internal standard to monitor the instrument stability and to determine the volume analysed

272   by the instrument. Flow cytometry analysis was used to test frustule isolation and to measure

273   prokaryotic presence in samples without additional prokaryotic counting.

274   **2.8. Statistical analysis.**

275   All analyses were performed with R (R Core Team, 2012), a freeware for statistical

276   analysis available at http://cran.r-project.org/. A Mann-Whitney *U* test was also used to test

277   the hypothesis H_0 that there is no difference between FA concentration averages during the

278   degradation experiment. We fixed the significance level at 5 %.

279   To compare the FA profiles of 'whole cells', 'extrenal' and 'frustule-associated'

280   fractions, a classical multidimensional scaling (MDS) was used on an Euclidean distance

281   matrix of FA standardised concentrations. Using k-means clustering, we partitioned our

282   samples into three groups. The number of clusters in this analysis must be defined by the

12

283   analyst. We choose three clusters because we have three sample types and also because it was

284   the result of the estimation by optimum average silhouette width using the fpc package in the

285   R software (Christian, 2010). Confident ellipses at 50 and 95 % were added to the plot to

286   represent results from cluster analysis and to comfort MDS observations.

287   **3. Results**

288   *3.1.*   **FA composition of *Thalassiosira weissflogii***

289

290   Whole cells (WC) fractions from two different cultures (B and C) had similar FA

291   compositions. The average composition (n = 6) was also similar to literature data on the same

292   genus (Table 1) and did not show obvious differences despite various methodologies used in

293   previous studies (Table 1). The composition of WC was dominated by palmitic acid 16:0

294   (26.4 ± 3.4 %, n = 6) (Table 1). The other dominant FA were those classically found in

295   diatoms: palmitoleic acid (16:1(n-7)) and eicosapentaenoic acid (20:5(n-3) or EPA) (18.3 ±

296   4.3 % and 22.5 ± 9.6 %, respectively). A characteristic feature was the dominance of 16-

297   carbon atom unsaturated FA compared to 18-carbon atom unsaturated FA (38.0 % versus 2.7

298   %, respectively) (Table 1). Also, 20:0 and 22:0 saturated FA were found in notably low

299   amounts (their sum was < 0.5 %), but their presence was confirmed by the analysis of their

300   mass spectra. Traces of heptadecanoic acid (17:0) and pentadecenoic acid (15:1) represented

301   less than 0.1 % of the total FA in WC. Those FA are generally attributed to prokaryotes

302   (Kaneda, 1991). Considering their low contribution to the total composition, the share of these

303   FA most likely reflected the presence of few bacteria. This scarcity was confirmed by flow

304   cytometry, which showed notably few microorganisms other than diatoms in the cultures (Fig.

305   2). Therefore, we did not take these bacterial markers into account in the FA profile of *T.*

306   *weissflogii*.

307   The 'external' fractions showed of the three cultures (A, B, and C), as for whole cells,

308   a dominance of 16:0, 16:1(n-7) and 20:5(n-3) FA (18.0 ± 4.4 %, 18.2 ± 3.2 % and 28.6 ± 6.8

309   %, respectively, n = 9) (Fig. 4). Taking into account the 16:2 and 16:3(n-4) FA, these FA

310   represented more than 85.9 % of the total FA for both WC and 'external' fractions.

311   The 'frustule-associated' fraction was dominated by saturated 14:0 and 16:0 FA (17.3

312   ± 5.9 % and 57.0 ± 4.9 %, respectively) (Fig. 4). This predominance of saturated FA led to a

313   lower contribution of other FA. Contrarily to the WC and 'external' fraction, unsaturated FA

314   with 16-carbon atoms were much less abundant in frustule-associated fraction (38.0 %, 41 %

315   and 10.8 % in WC, 'external' and 'frustule-associated' fractions, respectively) (Fig. 4).

316   Moreover, no branched nor 17:0 FA prokaryote markers were found in these fractions

317   emphasizing the non-contamination of 'frustule-associated' fraction. The major difference

318   with FA composition of the whole cell was the low degree of unsaturation of the FA from the

319   frustule.

320   Using k-means clustering method and MDS, comparison of FA profiles enabled to

321   identify three "groups": WC and 'external' fractions from culture A and B on the one hand,

322   WC and 'external' fractions from culture C on the other hand, and a third group composed of

323   'frustule-associated' fractions from all cultures (Fig. 5). The fact that A, B and C 'frustule-

324   associated' fractions were gathered together emphasized the specificity of frustule FA profiles

325   regardless of the culture conditions. The difference between culture C and the two other

326   cultures may be explained by a higher contribution and variability of 20:5(n-3) FA in culture

327   C in both 'external' and whole cells samples (Fig. 4), which were most probably related to the

328   different growth chamber (see section 2.1) or to a lag time for the sampling regarding the

329   growth curve.

14

3.2. Biotic degradation of diatom cells

Diatom material for the degradation experiment was obtained from the continuous reactor culture from Argenton. The overall degradation of the diatom material was reflected in the decrease of both POC and $bSiO_2$ concentrations over the 30-day incubation period (from 1480.2 to 496.6 ± 14.5 $\mu mol.l^{-1}$ and from 342.9 $\mu mol.l^{-1}$ to 76.4 ± 2.4 $\mu mol.l^{-1}$ for POC and $bSiO_2$, respectively) (Fig. 6). As expected, prokaryotes largely contributed to diatom decomposition, as shown by the increase in prokaryotic carbon during the first 4 days (Fig. 6). A total of 22 % of the initial $bSiO_2$ still remained in the batch at the end of the incubation experiment.

During the course of the degradation experiment, we focused on the kinetics of 'frustule-associated' FA and compared them with the kinetics of external lipids to highlight differences in degradation trends of the two fractions. External phytol and sterols represented 10.5 ± 3.2 % of the total external lipid pool (FA + Sterols + Phytol) at day 0. Their decrease over time from 17.7 ± 5.9 μmol $C.l^{-1}$ to below the detection limit at day 18 for phytol and from 18.0 ± 6.3 μmol $C.l^{-1}$ to 5.6 ± 0.8 $\mu molC.l^{-1}$ for sterols, well reflected the degradation of external algal material (Fig. 7). Total sterol concentrations exhibited an increase at day 6, mainly because of the analytical variability that was quite high between replicates, for the 24-methylene cholesterol in particular. We were not able to attribute this increase to any process. Interestingly, neither phytol nor sterols were detected in the 'frustule-associated' fraction. This observation and the fact that the internal standard (19:0) added to the pellet extraction medium has never been found in the 'frustule-associated' fraction confirmed that our protocol accurately separated these two fractions.

The saturated FA proportion (especially 18:0) of the 'external' fraction during degradation was higher than in cultures used to set up the protocol. Several factors may increase saturated FA in pellets. The culture used for degradation was more mature than

15

355 culture used to set up the protocol and proportions of unsaturated FA more susceptible to

356 oxidative attack than saturated ones, decrease in mature cells. Moreover, prokaryotes enriched

357 in saturated FA, were present in the culture medium at initial time of the degradation. In

358 addition to this, centrifugation used to sample the pellet for the degradation experiment

359 concentrates OM in general and not only diatoms. Thus, there was no possible interpretation

360 of the kinetics of degradation of external saturated FA. On the opposite, unsaturated FA that

361 dominated the FA in the diatom *Thalassiosira weissflogii* (50.7±6.5 % of Total FA) (Table 1)

362 are often used as markers of fresh diatom material (Balzano et al., 2011; Najdek et al., 2002).

363 They were proportionally less concentrated in the "degradation culture" (Table 2). However,

364 their decay over time (from 68.5 ± 27.5 µmol C.l^{-1} to 26.7 ± 10.2 µmol C.l^{-1} between days 0

365 and 30) (Fig. 7) and that of their individual components (Fig. 8) that characterized the algae in

366 both the WC and external fractions, namely C16:1n7, C16:2n4, C16:3n4, C18:1n7, C18:1n9,

367 C20:5n3 and C22:6n3 (Fig. 4), also reflected the prokaryotic degradation of the algal lipids.

368   At the beginning of the degradation experiment, saturated FA, 14:0, 16:0 and 18:0,

369 constituted the major part of the 'frustule-associated' FA (92.5 % of the total FA), as seen in

370 the diatom cultures (Fig. 3). The concentration of the frustule-associated saturated FA 14:0

371 and 16:0 did not exhibit significant differences over time (Fig. 9), whereas the concentration

372 of 18:0 decreased significantly after day 12 (Mann-Whitney U test, $p < 0.05$). This finding

373 suggested a different association with silica phases of the 18:0 compared to the 14:0 and 16:0.

374 Possibly, 18:0 was associated with a more soluble silica phase, the dissolution of this phase

375 being then necessary for 18:0 to be bioavailable. Unsaturated FA such as hexadecenoic acid

376 16:1 and oleic acid (18:1(n-9)) were still present in the frustule of *T. weissflogii* at the end of

377 incubation. More generally, these results were in line with a protective effect of the frustule

378 on its associated lipid fraction.

16

4. Discussion

4.1. **Evidence for frustule-associated fatty acids in *Thalassiosira weissflogii***

The FA composition of *Thalassiosira weissflogii* was similar to that reported in the literature for diatoms, with a predominance of 16:0, 16:1(n-7) and 20:5(n-3), which are often used as diatom markers (Dalsgaard et al., 2003) (Table 1). The proportions of saturated FA (approximately 35 %) were comparable to those found in the same species. Only few composition differences existed compared to results on the same species from Klein Breteler et al. (2005), with respect to unsaturated FA, especially the proportions of 16:1(n-7) and 20:5(n-3). This may come from differences in growth conditions (detailed in Table 1) known to impact physiological status and biochemical pools (Coombs et al., 1967; Vrieling et al., 1999).

In addition to these cellular lipids, our study showed that a significant pool of FA inaccessible to conventional lipid extraction technics was associated to the frustule of the diatom *Thalassiosira weissflogii*. It is now well established that existing interactions between the silica frustule and the organic matter depends on the diatom freshness or at the opposite of their burial period up to their fossilization in sediments. Breaking these interactions requires the use of either strong acids or oxidizing agents, either solvent. Depending on objectives, some protocols are adapted to the study of the silica content of the frustule and aim at denaturing and removing all organic material that it contains (Kamatani, 1971; Loucaides et al., 2008), others require the removal of silica to release organic matter (Bridoux and Ingalls, 2010; Ingalls et al 2003; Kröger et al 1994). In the latter case, the difficulty lies in preserving the integrity of the molecular structures after treatment of the sample. Recently, Morales et al. 2013 proposed a successful protocol to clean fresh diatoms for isotopic analysis of diatom

17

403 frustule-bound nitrogen. However, the harsh oxidative treatment transformed all organic

404 nitrogen into nitrates preventing analysis of biochemical groups and molecular structures.

405   To our knowledge the first characterisation of a lipid pool embedded into the frustules

406 of *T. weissflogii* was done by using nuclear magnetic resonance on SDS/EDTA/H_2O_2

407 extracted frustules of *T. pseudonana* by Tesson et al. (2008). Their results indicated the

408 presence of C=C from double bonds, -(CH_n)- from aliphatic chains and C=O from carbonyl

409 groups of FA. Previously, Kates and Volcani (1968) were the first to strongly demonstrate a

410 lipid/frustule association in seven marine diatom species and to analyse FA. These authors

411 washed frustules using distilled water and they added, after a Bligh and Dyer lipid extraction,

412 a methanolic-HCl step to cleave bound-lipids. As such, the cell wall lipid composition was

413 likely dominated by cellular material together with externally bound-lipids as no silica

414 dissolution step was included in the protocol, as shown by our experiment in which fatty acid

415 composition of external fraction was mainly identical to the fatty acid composition of the

416 whole cell.

417   In our study, we pushed a step further the protocol of Kate and Volcani by adding an

418 hot NaOH silica dissolution step after the first B&D extraction of washed fragmented diatom

419 pellets. Briefly, in our protocol, frustule pellets were isolated from the cellular material by

420 sequential washings and centrifugation of fragmented diatoms in pure water followed by a

421 B&D extraction of external lipids. Then, silica frustules were dissolved with NaOH (1mol. l^{-1})

422 and re-extracted at acidic pH by dichloromethane solvent to obtain the frustule-associated

423 lipids.

424   Long chain carboxylic acids are major constituents of diatom lipids. They are free or

425 esterified to glycerol, to other alcohols, or to more complex glycosidic and phosphatidic

426 moieties. After sonication and water washing treatments, a fraction of the cellular lipids

427 remained attached to the silica frustule through either hydrogen bonding, or electrostatic and

428   hydrophobic interactions with other molecules constitutive of the cell wall. This was

429   confirmed by the flow cytometry analysis of frustule pellets showing chla after cells

430   fragmentation and washings.

431   The B&D protocol was particularly suitable to remove the lipid external fraction with

432   preservation of intact molecular structures. The monophasic solvent extraction mixture

433   (chloroform/methanol/0.1M NaCl in water) is a powerful extracting agent for both disruption

434   of these bonding's and lipid dissolution (Kates, 1986), while the second step through addition

435   of proper amounts of chloroform and water, achieves an efficient separation of hydrophobic

436   and hydrophilic compounds by changing the monophasic mixture into biphasic. The NaOH

437   treatment of frustules free from the external organic material gives access to the organic

438   matter associated to the silica matrix. Not only NaOH increases silica dissolution but it is

439   widely use to cleave hydrogen and covalent bonds, which favour separation of FA from the

440   silica phase and most probably from the organic matrix that may be present. We did not use

441   oxidizing agent such as perchloric acid suitable for the extraction of aqueous metabolites

442   (Ingalls et al. 2009) as it has a deleterious effect on lipid components. We tested the use of HF

443   to dissolve silica but precautions required for its use (plastic or polypropylene containers)

444   makes its use incompatible with the analysis of lipids.

445   The efficiency of our protocol for isolating and extracting frustule-associated lipids

446   was demonstrated first by the absence of cellular compounds (i. e. phytol and sterols) in

447   frustule-associated lipids, secondly by the fact that the internal standard (19:0) added to the

448   cellular fraction was not recovered with the frustule-associated lipid fraction (see section 2.4)

449   and finally, because FA markers of prokaryotes that contributed for a few percent of the

450   pellets total carbon were also absent from the frustule-associated lipids. In addition, we used

451   our isolation/extraction protocol at different stages of dissolution of the silica phases during a

452   bacterial degradation experiment of these diatoms. Frustule-associated FA thus extracted were

19

453 found similar to that of frustule-associated FA in fresh *Thalassiosira weissflogii* diatom

454 culture validating our protocole and showing little accessibility of these FA to degradation.

455   External FA were identified as cellular lipids because of their composition similar to

456 that of FA in whole cells. While results did not show any specific FA marker of the frustule,

457 frustule-associated FA were characterised by a very low degree of unsaturation with

458 predominance of14:0, 16:0 and 18:0 FA. Although high pH (NaOH 1 mol.l^{-1}) and the absence

459 of chlorophyll favour neither autoxidation nor photooxidation (Petit et al., 2013; Rontani,

460 2001), the reactivity of unsaturated FA to oxidation could have led to a decrease of

461 unsaturation degree due to experimental conditions and extraction process. However, tests to

462 determine the effect of temperature (70 °C) on polyunsaturated FA (20:4(n-6)), and previous

463 observations that report unsaturated FA conservation during hot saponification (> 100 °C, see

464 section 2.7.1), suggest that our protocol had little effect on FA unsaturation. Oleic acid

465 (18:1(n-9)) and the unidentified 16:1 FA were present in the 'frustule-associated' fraction

466 isolated from *T. weissflogii* cultures, even after 30 days of degradation. Thus, 16:1 and 18:1

467 FA may likely be associated to a resistant to degradation/dissolution phase of organic or silica

468 matrices.

469   The very strong similarity between FA profiles of frustules of the different cultures

470 (Fig. 5), although clear differences appeared for others fractions, indicated that 'frustule-

471 associated' FA were less sensitive to growth conditions than cellular FA. Nevertheless, the

472 study of Soler et al. (2010) shows an effect of nutrient starvations, especially phosphorus

473 starvation, on the FTIR- analysed biochemical composition of *T. weissflogii* frustule. These

474 authors suggested that biochemical changes lead to frustule structure changes leading *in fine*

475 to changes in bSiO$_2$ dissolution. Therefore, although frustule-associated FA in sediments may

476 not be used as markers of nutrient regime during paleoproduction, changes in other

477 biochemical fractions should be considered when studying frustules in deep sediments.

478   Kates and Volcani (1968) suggested that lipids could be distributed according to their

479   unsaturation level in the frustule. The degradation of the 18:0 and some unsaturated FA

480   (16:1(n-7), 18:2(n-6), 20:4(n-6) and 20:5(n-3)) of the frustule while 14:0 and 16:0 were

481   almost not degraded at all is in agreement with a non-homogenous association of FA with the

482   frustule. These results also confirm the existence of different organic pools in the silica matrix

483   of the frustules (Abramson et al., 2009; Tesson et al. 2008, 2013) and of different silica

484   phases associated with different pool of organic matter (Moriceau et al., 2009). Using a

485   spectroscopic method, Abramson et al. (2009) concluded that the OM encased within the

486   structure of the frustule, which is resistant to different chemical attacks, may be protected

487   from decomposition until the release of this matter into the surrounding environment occurs.

488   This last method advantageously allowed locating the organic pools in *Cylindrotheca*

489   *fusiformis* because of its thin frustule. However it is not valid to accurately quantify organic

490   pools and it can hardly be adapted to other species as thicker frustules absorb X-rays too

491   strongly. In contrast, our methodology may be used to quantify the pool of FA embedded in

492   the frustule of a large choice of diatom species.

493

494   **4.2.   Implications for the export of organic matter**

495   In some cases, huge numbers of fresh diatom cells can sink out of the euphotic layer

496   (Martin et al., 2011), carrying with them different pool of organic matter; extra-, intra-cellular

497   and intra-frustule. On the contrary to what was previously thought, the fraction of organic

498   matter embedded or associated to the frustule could be an important fraction of the total POC

499   (1.8 % of the diatom POC in surface water and up to 5.8 % of the diatom POC after 30 days

500   of degradation).

501   To better understand the implication of this result in term of export, we compared our

502   experimental data to the *in situ* data compiled by Ragueneau et al. (2002). More precisely,

21

503 data from the Northern Antarctic Circumpolar Current site (NACC) were used for comparison

504 because $bSiO_2$ dissolution at this site (82 % of $bSiO_2$ dissolution at 4224 m depth) was

505 comparable to the final dissolution measured in our degradation/dissolution experiment (78 %

506 of our initial $bSiO_2$ after 30 days incubation). The 'frustule-associated' FA represented 5.8 %

507 of the total POC at the end of our experiment. The amount of these 'frustule-associated' FA

508 for each mol of $bSiO_2$ after 78 % of dissolution was 0.23 molC FA.mol $bSiO_2^{-1}$. Assuming

509 that 14:0 and 16:0 FA are associated to the less soluble phase of the frustule without

510 excluding possible association with the organic matrix, the flux of the 'frustule-associated' FA

511 at 4224 m may be estimated from the $bSiO_2$ flux (0.14 $mol.m^{-2}.yr^{-1}$) found at this site. This

512 calculated 'frustule-associated' FA flux amounted to 0.0322 $molC.m^{-2}.yr^{-1}$ which represents 64

513 % of the POC flux at 4224 m at NACC site. When N in frustules is on the order of 15 µmol

514 N/g opal and the C associated with amino acids is also reported in units of µmol C/g (Ingalls

515 et al., 2010), this calculation suggests that our protocol extracts frustule-bound fatty acids and

516 another FA fraction not embedded but strongly associated to the frustule and the organic

517 matrix.

518   Keeping in mind the limitation of this comparison, especially in terms of the species

519 studied (low latitude widespread species) and experimental conditions that did not consider *in*

520 *situ* conditions (temperature, pressure, grazing) our study still raises the possible importance

521 of the contribution of 'frustule-associated' FA to the organic carbon flux. According to our

522 simple calculation, these 'frustule-associated' FA could represent an important part of the

523 POC reaching the sediment. Interestingly, this assessment is in line with the correlation

524 observed at depth between the sedimentation flux of POC and the sedimentation flux of $bSiO_2$

525 as revealed by the study of Armstrong et al. (2009, 2002), Francois et al. (2002), Klaas and

526 Archer (2002) and Ragueneau et al. (2006).

527   In further studies of sinking particles and sediments, a more systematic

528   hydrolysis/dissolution of deep samples should be used to consider this intra-frustule organic

529   matter and to correctly estimate the sedimentation of the different organic pools. Until now,

530   the different protocol used showed that this fraction is taken into account when measuring

531   total POC but not when characterizing the different organic pools. As such, this fraction

532   could be part of the large uncharacterized organic matter pool at depths (Wakeham, 1995).

533   As shown by our degradation/dissolution results, the 'frustule-associated' organic

534   matter is not available to prokaryotes before the complete frustule dissolution. As a result and

535   because of the saturation in dissolved silicon in interstitial water in bottom sediments (Van

536   Cappellen, 2002), its release in sediments should be slower than previously thought and could

537   not be a valuable source of energy for the organisms feeding on the seafloor. Another point of

538   interest is the better preservation of lipids in sediments and their usefulness as biomarkers in

539   paleoceanographic studies (Wakeham, 1995). The fact that sterols are not found embedded in

540   the frustule of *T. weissflogii*, although many deep sediment analysis reveal their presence

541   (Wakeham et al., 1997), could be used to estimate the proportion of intracellular versus

542   'frustule-associated' organic carbon in opal dominated sediments.

543   *Conclusion*

544   Our study suggests an interesting and effective protocol to approach the FA

545   composition of the organic matter embedded in or strongly associated to the frustule. Clear

546   differences exist between the FA composition of the whole cell and the FA composition of the

547   OM embedded and associated to the frustule which are characterised by a very low degree of

548   unsaturation. Moreover, FA composition of the whole cell seem a lot more sensitive to small

549   differences in the growth conditions than FA associated to the frustule. When *T. weissflogii*

550   underwent a 30 days degradation, the FA associated to the frustule represented 5.8 % of the

551   remaining POC suggesting the importance of their role in carbon export. With our study we

23

552 infer that organic matter associated to the frustule or embedded in the frustule may be

553 consider when investigating carbon export. This pool could partially explain the correlation

554 observed at depth between Si and C sedimentation fluxes despite the decoupling between

555 $bSiO_2$ dissolution and POC degradation processes.

564 *References*

565 Abramson, L., Wirick, S., Lee, C., Jacobsen, C.J., Brandes, J.A., 2009. The use of soft X-ray
566   spectromicroscopy to investigate the distribution and composition of organic matter in a
567   diatom frustule and a biomimetic analog. Deep Sea Research Part II - Topical Studies in
568   Oceanography 56, 1369–1380.

569 Armstrong, R.A., Lee, C., Hedges, J.I., Honjo, S., Wakeham, S.G., 2002. A new, mechanistic
570   model for organic carbon fluxes in the ocean based on the quantitative association of
571   POC with ballast minerals. Deep Sea Research Part II - Topical Studies in Oceanography
572   49, 219–236.

573 Armstrong, R.A., Peterson, M.L., Lee, C., Wakeham, S.G., 2009. Settling velocity spectra and
574   the ballast ratio hypothesis. Deep Sea Research Part II: Topical Studies in Oceanography
575   56, 1470–1478.

576 Balzano, S., Pancost, R.D., Lloyd, J.R., Statham, P.J., 2011. Changes in fatty acid
577   composition in degrading algal aggregates. Marine Chemistry 124, 2–13.

578 Bidle, K.D., Azam, F., 1999. Accelerated dissolution of diatom silica by marine bacterial
579   assemblages. Nature 397, 508–512.

580   Bridoux, M.C., Annenkov, V. V, Keil, R.G., Ingalls, A.E., 2012. Widespread distribution and
581   molecular diversity of diatom frustule bound aliphatic long chain polyamines (LCPAs)
582   in marine sediments. Organic Geochemistry 48, 9–20.

583   Bridoux, M.C., Ingalls, A.E., 2010. Structural identification of long-chain polyamines
584   associated with diatom biosilica in a Southern Ocean sediment core. Geochimica et
585   Cosmochimica Acta 74, 4044–4057.

586   Brunner, E., Gröger, C., Lutz, K., Richthammer, P., Spinde, K., Sumper, M., 2009. Analytical
587   studies of silica biomineralization: towards an understanding of silica processing by
588   diatoms. Applied Microbiology and Biotechnology 84, 607–16.

589   Buesseler, K.O., 1998. The decoupling of production and particulate export in the surface
590   ocean. Global Biogeochemical Cycles 12, 297–310.

591   Chen, X., Wakeham, S.G., Fisher, N.S., 2011. Influence of iron on fatty acid and sterol
592   composition of marine phytoplankton and copepod consumers. Limnology and
593   Oceanography 56, 716–724.

594   Chiovitti, A., Harper, R.E., Willis, A., Bacic, A., Mulvaney, P., Wetherbee, R., 2005.
595   Variations in the substituted 3-linked mannans closely associated with the silicified walls
596   of diatoms. Journal of Phycology 41, 1154–1161.

597   Christian, H., 2010. fpc: Flexible procedures for clustering. R package version 2.0-2.
598   http://CRAN.R-project.org/package=fpc.

599   Coombs, J., Darley, W.M., Holm-Hansen, O., Volcani, B.E., 1967. Studies on the
600   biochemistry and fine structure of silica shell formation in diatoms. Chemical
601   composition of Navicula pelliculosa during silicon-starvation synchrony. Plant
602   Physiology 42, 1601–6.

603   Dalsgaard, J., St John, M.A., Kattner, G., Müller-Navarra, D., Hagen, W., 2003. Fatty acid
604   trophic markers in the pelagic marine environment. Advances in Marine Biology 46,
605   225–340.

606   De La Rocha, C.L., Passow, U., 2007. Factors influencing the sinking of POC and the
607   efficiency of the biological carbon pump. Deep Sea Research Part II - Topical Studies in
608   Oceanography 54, 639–658.

609   Falkowski, P.G., Barber, R.T., Smetacek, V., 1998. Biogeochemical controls and feedbacks
610   on ocean primary production. Science 281, 200–206.

611   Fileman, T.W., Pond, D.W., Barlow, R.G., Mantoura, R.F.C., 1998. Vertical profiles of
612   pigments, fatty acids and amino acids: Evidence for undegraded diatomaceous material
613   sedimenting to the deep ocean in the Bellingshausen Sea, Antarctica. Deep Sea Research
614   Part I - Oceanographic Research Papers 45, 333–346.

615   François, R., Honjo, S., Krishfield, R., Manganini, S., 2002. Factors controlling the flux of
616   organic carbon to the bathypelagic zone of the ocean. Global Biogeochemical Cycles 16,
617   1087.

618 Gordon, L.I., Jennings, J.C., Ross, A.A., Krest, J.M., 1993. A suggested protocol for
619   continuous flow automated analysis of seawater nutrients (phosphate, nitrate, nitrite and
620   silicic acid) in the WOCE Hydrographic Program and the Joint Global Ocean Fluxes
621   Study. WHP Operations and Methods. WOCE Hydrographic Program Office. Methods
622   manual 19–1.

623 Goutx, M., Wakeham, S.G., Lee, C., Duflos, M., Guigue, C., Liu, Z., Moriceau, B., Sempéré,
624   R., Tedetti, M., Xue, J., 2007. Composition and degradation of marine particles with
625   different settling velocities in the northwestern Mediterranean Sea. Limnology and
626   Oceanography 52, 1645–1664.

627 Guillard, R.R.L., Ryther, J.H., 1962. Studies of marine planktonic diatoms : I. Cyclotella nana
628   Hustedt, and Detonula confervacea (Cleve) Gran. Canadian Journal of Microbiology 8,
629   229–239.

630 Hedges, J.I., Baldock, J.A., Gélinas, Y., Lee, C., Peterson, M.L., Wakeham, S.G., 2001.
631   Evidence for non-selective preservation of organic matter in sinking marine particles.
632   Nature 409, 801–804.

633 Hildebrand, M., 2003. Biological processing of nanostructured silica in diatoms. Progress in
634   Organic Coatings 47, 256–266.

635 Hildebrand, M., 2008. Diatoms, biomineralization processes, and genomics. Chemical
636   reviews 108, 4855–74.

637 Hildebrand, M., Holton, G., Joy, D.C., Doktycz, M.J., Allison, D.P., 2009. Diverse and
638   conserved nano- and mesoscale structures of diatom silica revealed by atomic force
639   microscopy. Journal of Microscopy 235, 172–87.

640 Ingalls, A.E., Whitehead, K., Bridoux, M.C., 2010. Tinted windows: The presence of the UV
641   absorbing compounds called mycosporine-like amino acids embedded in the frustules of
642   marine diatoms. Geochimica et Cosmochimica Acta 74, 104–115.

643 Kamatani, A., 1971. Physical and chemical characteristics of biogenous silica. Marine
644   Biology 95.

645 Kamatani, A., Riley, J.P., 1979. Rate of dissolution of diatom silica walls in seawater. Marine
646   Biology 55, 29–35.

647 Kates, M., Volcani, B.E., 1968. Studies on the biochemistry and fine structure of silica shell
648   formation in diatoms. Lipid components of the cell walls. Z. Pflanzenphysiol 19–29.

649 Klaas, C., Archer, D.E., 2002. Association of sinking organic matter with various types of
650   mineral ballast in the deep sea: Implications for the rain ratio. Global Biogeochemical
651   Cycles 16.

652 Klein Breteler, W.C.M., Schogt, N., Rampen, S.W., 2005. Effect of diatom nutrient limitation
653   on copepod development: the role of essential lipids. Marine Ecology Progress Series
654   291, 125–133.

26

655 Kröger, N., Bergsdorf, C., Sumper, M., 1994. A new calcium binding glycoprotein family
656   constitutes a major diatom cell wall component. The EMBO journal 13, 4676–4683.

657 Kröger, N., Deutzmann, R., Sumper, M., 1999. Polycationic peptides from diatom biosilica
658   that direct silica nanosphere F formation. Science 286, 1129–1132.

659 Kröger, N., Lehmann, G., Rachel, R., Sumper, M., 1997. Characterization of a 200-kDa
660   diatom protein that is specifically associated with a silica-based substructure of the cell
661   wall. European Journal of Biochemistry 250, 99–105.

662 Kröger, N., Lorenz, S., Brunner, E., Sumper, M., 2002. Self-assembly of highly
663   phosphorylated silaffins and their function in biosilica morphogenesis. Science 298,
664   584–6.

665 Kucki, M., 2009. Biological Photonic Crystals: Diatoms. PhD Thesis. University of Kassel.
666   Department of Natural Science pp 166.

667 Loucaides, S., Van Cappellen, P., Behrends, T., 2008. Dissolution of biogenic silica from land
668   to ocean: Role of salinity and pH. Limnology and Oceanography 53, 1614–1621.

669 Mann, D.G., Droop, S.J.M., 1996. 3. Biodiversity, biogeography and conservation of diatoms.
670   Hydrobiologia 336, 19–32.

671 Martin, P., Lampitt, R.S., Jane Perry, M., Sanders, R., Lee, C., D'Asaro, E., 2011. Export and
672   mesopelagic particle flux during a North Atlantic spring diatom bloom. Deep Sea
673   Research Part I - Oceanographic Research Papers 58, 338–349.

674 Martin-Jézéquel, V., Hildebrand, M., Brzezinski, M.A., 2000. Silicon metabolism in diatoms :
675   implications for growth. Journal of Phycology 36, 821–840.

676 Moriceau, B., Goutx, M., Guigue, C., Lee, C., Armstrong, R.A., Duflos, M., Tamburini, C.,
677   Charrière, B., Ragueneau, O., 2009. Si–C interactions during degradation of the diatom
678   Skeletonema marinoi. Deep Sea Research Part II - Topical Studies in Oceanography 56,
679   1381–1395.

680 Mullin, J.B., Riley, J.P., 1955. The colorimetric determination of silicate with special
681   reference to sea and natural waters. Analytica Chimica Acta 12.

682 Najdek, M., Debobbis, D., Miokovic, D., Ivancic, I., 2002. Fatty acid and phytoplankton
683   compositions of different types of mucilaginous aggregates in thenorthern Adriatic.
684   Journal of Plankton Research 24, 429–441.

685 Nelson, D.M., Tréguer, P., Brzezinski, M.A., Leynaert, A., Quéguiner, B., 1995. Production
686   and dissolution of biogenic silica in the ocean : Revised global estimates , comparison
687   with regional data and relationship to biogenic sedimentation. Global Biogeochemical
688   Cycles 9, 359–372.

689 Patrick, S., Holding, A.J., 1985. The effect of bacteria on the solubilization of silica in diatom
690   frustules. Journal of Applied Microbiology 7–16.

691   Petit, M., Sempéré, R., Vaultier, F., Rontani, J.-F., 2013. Photochemical production and
692   behavior of hydroperoxyacids in heterotrophic bacteria attached to senescent
693   phytoplanktonic cells. International Journal of Molecular Sciences 14, 11795–11815.

694   R Core Team, 2012. R: A language and environment for statistical computing. R Foundation
695   for Statistical Computing, Vienna, Austria.

696   Ragueneau, O., Dittert, N., Pondaven, P., Tréguer, P., Corrin, L., 2002. Si/C decoupling in the
697   world ocean: is the Southern Ocean different? Deep Sea Research Part II - Topical
698   Studies in Oceanography 49, 3127–3154.

699   Ragueneau, O., Schultes, S., Bidle, K.D., Claquin, P., Moriceau, B., 2006. Si and C
700   interactions in the world ocean: Importance of ecological processes and implications for
701   the role of diatoms in the biological pump. Global Biogeochemical Cycles 20, 1–15.

702   Ragueneau, O., Tréguer, P., 1994. Determination of biogenic silica in coastal waters:
703   applicability and limits of the alkaline digestion method. Marine Chemistry 45, 43–51.

704   Raven, J.A., Waite, A.M., 2004. The evolution of silicification in diatoms: inescapable
705   sinking and sinking as escape? New Phytologist 162, 45–61.

706   Rontani, J.-F., 2001. Visible light-dependent degradation of lipidic phytoplanktonic
707   components during senescence: a review. Phytochemistry 58, 187–202.

708   Rontani, J.-F., Zabetti, N., Wakeham, S.G., 2011. Degradation of particulate organic matter in
709   the equatorial Pacific Ocean: Biotic or abiotic? Limnology and Oceanography 56, 333–
710   349.

711   Soler, C., Claquin, P., Goutx, M., Ragueneau, O., Moriceau, B., 2010. Impact of nutrient
712   starvation on the biochemical composition of the marine diatom Thalassiosira
713   weissflogii: from the whole cell to the frustule fraction. Biogeosciences Discussions 7,
714   5953–5995.

715   Tesson, B., Hildebrand, M., 2013. Characterization and localization of insoluble organic
716   matrices associated with diatom cell walls: Insight into their roles during cell wall
717   formation. PloS one 8, e61675.

718   Tesson, B., Masse, S., Laurent, G., Maquet, J., Livage, J., Martin-Jézéquel, V., Coradin, T.,
719   2008. Contribution of multi-nuclear solid state NMR to the characterization of the
720   Thalassiosira pseudonana diatom cell wall. Analytical and Bioanalytical Chemistry 390,
721   1889–1898.

722   Thornton, D.C.O., 2002. Diatom aggregation in the sea: mechanisms and ecological
723   implications. European Journal of Phycology 37, 149–161.

724   Tréguer, P., Le Corre, P., 1975. Manuel d'analyse des sels nutritifs dans l'eau de mer.
725   Utilisation de l'autoanalyseur II Technicon. Université de Bretagne Occidentale, Brest.

726   Turner, J.T., 2002. Zooplankton fecal pellets, marine snow and sinking phytoplankton
727   blooms. Aquatic Microbial Ecology 27, 57–102.

728   Van Cappellen, P., 2002. Biogenic silica dissolution in the oceans: Reconciling experimental
729   and field-based dissolution rates. Global Biogeochemical Cycles 16.

730   Volk, T., Hoffert, M.I., 1985. Ocean carbon pumps: Analysis of relative strengths and
731   efficiencies in ocean-driven atmospheric CO2 changes, in: Sunquist, E.T., Broecker,
732   W.S. (Eds.), The Carbon Cycle and Atmospheric CO2: Natural Variations Archean to
733   Present. American Geophysical Union, Washington, DC, pp. 99–110.

734   Volkman, J.K., Hallegraeff, G.M., 1988. Lipids in marine diatoms of the genus Thalassiosira :
735   Predominance of 24-methylenecholesterol. Phytochemistry 27, 1389–1394.

736   Vrieling, E., Poort, L., Beelen, T., 1999. Growth and silica content of the diatoms
737   Thalassiosira weissflogii and Navicula salinarum at different salinities and enrichments
738   with aluminium. European Journal of Phycology 307–316.

739   Wakeham, S.G., 1995. Lipid biomarkers for heterotrophic alteration of suspended particulate
740   organic matter in oxygenated and anoxic water columns of the ocean. Deep Sea Research
741   Part I - Oceanographic Research Papers 42, 1749–1771.

742   Wakeham, S.G., Lee, C., Hedges, J.I., Hernes, P.J., Peterson, M.L., 1997. Molecular
743   indicators of diagenetic status in marine organic matter. Geochimica et Cosmochimica
744   Acta 61, 5363–5369.

745

746

Table 1. Fatty Acid (FA) compositions (mol %) of diatoms from the *Thalassiosira*

748 genus.

	T. pseudonana[1]	*T. pseudonana*[2*]	*T. pseudonana*[2§]	*T. oceanica*[2*]	*T. oceanica*[2§]	*T. weissflogii*[3α]	*T. weissflogii*[3β]	*T. weissflogii*[4]
Saturates								
12:0	Tr	-	-	-	-	-	-	-
14:0	14.3	3.5	6.1	18.4	10.0	9.1	8.5	6.2
15:0	0.8	0.6	1.0	1.6	1.1	1.3	1.3	0.9
16:0	11.2	18.4	26.9	23.0	23.7	28.3	26.4	26.4
17:0	0.1	-	-	-	-	-	-	-
18:0	0.7	1.6	1.4	0.3	1.0	1.1	0.2	0.9
20:0	0.1	1.1	0.3	-	-	-	-	0.2
22:0	Tr	-	-	-	-	-	-	0.1
24:0	Tr	-	-	-	-	0.1	0.1	0.1
Sum %	27.2	25.2	35.7	43.3	35.8	39.9	36.5	34.8
Mono-UNS								
16:1(n-13)t	0.4	Tr	-	0.5	-	0.4$^\Omega$	0.3$^\Omega$	-
16:1(n-7)	18.0	21.0	32.0	30.0	25.8	40.5	40.8	18.3
16:1(n-5)	0.3	1.6	Tr	Tr	0.2	0.6$^\Omega$	0.7$^\Omega$	0.8$^\varphi$
18:1(n-9)	0.5	2.0	1.5	0.5	5.0	0.5	0.5	0.5
18:1(n-7)	0.1	0.1	0.2	4.0	Tr	0.2	0.1	0.6
20:1(n-9)	0.2	-	-	-	-	-	-	Tr
24:1	-	-	-	-	-	0.3	0.1	0.1$^\varphi$
Sum %	19.5	24.7	33.7	35.0	31.0	41.2	41.4	20.3
Poly-UNS								
16:2(n-7)	2.7	1.1	1.8	0.7	-	-	-	-
16:2(n-4)	4.5	0.7	1.4	1.4	-	-	-	6.6$^\varphi$
16:3(n-4)	12.7	7.1	4.8	3.5	6.4	5.8$^\Omega$	6.6$^\Omega$	12.3
16:4(n-1)	2.3	2.3	0.8	0.8	3.9	-	-	-
18:2(n-9)	Tr	-	-	-	-	-	-	-
18:2(n-6)	0.4	1.8	1.3	1.0	1.1	0.7	0.6	0.2
18:3(n-6)	0.2	-	-	-	-	-	-	-
18:3(n-3)	0.1	0.8	0.7	1.1	0.9	-	-	-
18:4(n-3)	5.3	5.8	4.0	1.8	5.2	2.6	3.1	1.4
20:4(n-6)	0.3	1.1	0.9	Tr	Tr	θ	θ	Tr
20:4(n-3)	0.3	-	-	-	-	-	-	-
20:5(n-3)	19.3	23.9	12.1	11.0	13.4	7.4	9.6	22.5
22:6(n-3)	3.9	3.5	1.5	1.4	0.8	0.9	0.1	1.9
Sum %	52.0	48.1	29.3	22.7	31.7	11.9	13.5	44.9
other	1.3	2.0	1.3	0.4	1.5	0.3	0.1	-
Total	100.0	100.0	100.0	101.4	100.0	100.1	99.1	100.0

749 [1]From Volkman et al. (1989). Culture was made in G/2 medium and with a 12hr/12hr light/dark cycle at 20 °C.
750 [2]From Volkman and Hallegraeff (1988). FA were analyzed in free fatty acids[*] and triacylglycerols[§] separately in
751 two different species grown in f/2 medium (enriched with Na-EDTA for T. oceanica) and with a 12hr/12hr light/dark cycle at
752 17.5 °C.
753 [3]From Klein Breteler et al. (2005). Their results are presented from two separated continuous cultures of *T.*
754 *weissflogii* ([3α] and [3β]) grown on f/2 medium and with a 16hr/8hr light dark cycle at 15 °C. $^\Omega$Double bond position is not

755 indicated for three FA: 16:1, 16:1 and 16:3. For a convenient presentation, we assume their identity according to their
756 contribution. [θ]Two FA, 20:4(n-6) and 20:5(n-3), are pooled in their study.
757 [4]From this study (average of two independent cultures). [φ]In our study, the position of some double bonds are not
758 localized.
759 Tr = Trace<0.05% as we assume in Volkman and Hallegraeff (1988). For non detected FA, a – is indicated. UNS =
760 unsaturated.

31

761   Table 2. FA compositions (mol %) of *Thalassiosira weissflogii* in this study.

		T.weissflogii[a]	*T.weissflogii* for degradation[b]
Saturates			
	14:0	6.2	4.2
	15:0	0.9	2.1
	16:0	26.4	37.3[*]
	18:0	0.9	32.5[*]
	20:0	0.2	0.9
	22:0	0.1	-
	24:0	0.1	0.4
Sum %		34.8	77.4
Mono-UNS			
	16:1 (n-7)	18.3	4.0
	16:1	0.8	1.0
	16:1 φ	-	0.3[φ]
	18:1 (n-9)	0.5	2.6
	18:1 (n-7)	0.6	2.3
	20:1 (n-9)	Tr	-
	24:1	0.1	-
Sum %		20.3	10.2
Poly-UNS			
	16:2	6.6	1.4
	16:3 (n-4)	12.3	1.6
	18:2 (n-6)	0.2	0.7
	18:4 (n-3)	1.4	-
	20:3	-	0.3
	20:4 (n-6)	Tr	0.4
	20:5 (n-3)	22.5	5.9
	22:6 (n-3)	1.9	2.1
Sum %		44.9	12.4
Total		100.0	100.0

762   [a]FA composition at the end of the growth phase (average of the two cultures, n = 6).
763   [b]FA composition at the beginning of the degradation experiment (n = 3).
764   [*]Some FA bacterial markers were found in lipid extracts from degradation experiment samples (15:0iso,
765 15:0anteiso and 17:0). We choose to not take them into account and keep the composition found during growth of *T.*
766 *weissflogii*. However, it is clear that other FA such as palmitic and stearic acids are shared by diatoms and bacteria.
767   [φ]Another 16:1 FA was found in FA profiles but the position of its double bond was not localized.

32

769   Figure 1. Schematic representation showing the different steps of the protocol. Cells
770 are broken using hot sonication and centrifuged three times with milli$Q$ water to remove
771 intracellular material. Pellets of fragmented frustules are then extracted using organic solvents
772 following the Bligh and Dyer protocol (B&D). The organic phase contains the external
773 fraction. Frustules accumulated at the interface form a "white layer" composed of washed
774 frustules (see photo of scanning electron microscopy). Frustules are dissolved with NaOH 1M
775 at 95°C to release frustule-associated fraction that is further extracted with CH_2Cl_2 at pH<2.
776   Figure 2. Cytograms of whole cells (A) and isolated frustules after three
777 centrifugations with 40 ml of Milli$Q$ water (B). Cytograms represent the chlorophyll
778 fluorescence of particles function of their granularity (side scatter). Some frustules still show
779 fluorescence of chlorophyll molecules indicating presence of external material.
780   Figure 3. Frustules fragments of *Thalassiosira weissflogii* freed from their "external
781 fraction" observed in scanning electron microscopy.
782   Figure 4. Relative FA compositions of whole cells, external and frustule-associated
783 fractions. All samples are gathered under each bar by averaging the FA contribution in each
784 culture. n = 6 for whole cells (culture B and C) and n = 9 for the two other fractions (cultures
785 A, B and C). Error bars represent the standard deviation.
786   Figure 5. Graphical representation of the classical multidimensional scaling analysis of
787 whole cells samples (black diamonds), external fractions (grey dots) and frustule-associated
788 fractions (white triangles). Confident ellipses containing 50 and 95% of the data used to build
789 clusters obtained from *k*-means analysis are represented.
790   Figure 6. Evolution of concentrations of total POC (black dots), bacterial OC (black
791 squares), and biogenic silica ($bSiO_2$, grey triangles) during the course of the degradation
792 experiment. Solid and dashed lines represent averaged value for each parameter. OC
793 (particulate and bacterial) and $bSiO_2$ concentrations are expressed as $\mu mol.l^{-1}$. For a
794 convenient representation, the y axis for $bSiO_2$ concentration is on the right of the graph.
795   Figure 7. Concentrations ($\mu molC.l^{-1}$) of total unsaturated FA (black dots and solid

796 line), total sterols (black diamonds and dashed line) and phytol (grey squares and line) in

797 external fractions at each sampling day during the course of the degradation experiment. Error

798 bars represent standard deviation (n = 3). After day 12, phytol concentrations were under
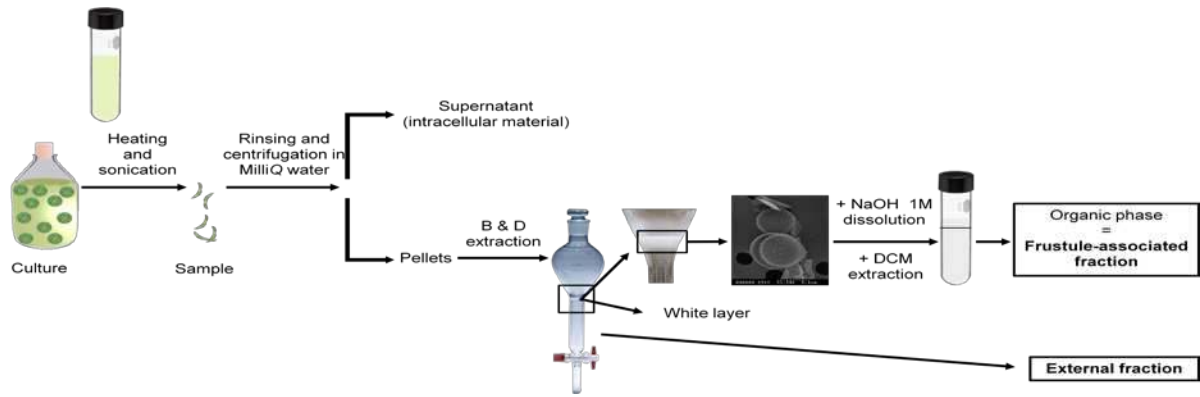
799 detection limit. At day 18, n=1.

800   Figure 8. Concentrations ($\mu molC.l^{-1}$) of individual unsaturated FA characteristic of
801 external fractions at each sampling day during the course of the degradation experiment. Error
802 bars represent standard deviation (n = 3). At day 18 and 30, n = 1.
803   Figure 9. Mean concentrations ($\mu molC.l^{-1}$) of total FA (dots and solid line), saturated

804 14:0 (triangles and dotted line), 16:0 (diamonds and long-dashed line) and 18:0 (squares and

805 short-dashed line) in frustule-associated material during the degradation. Error bars represent

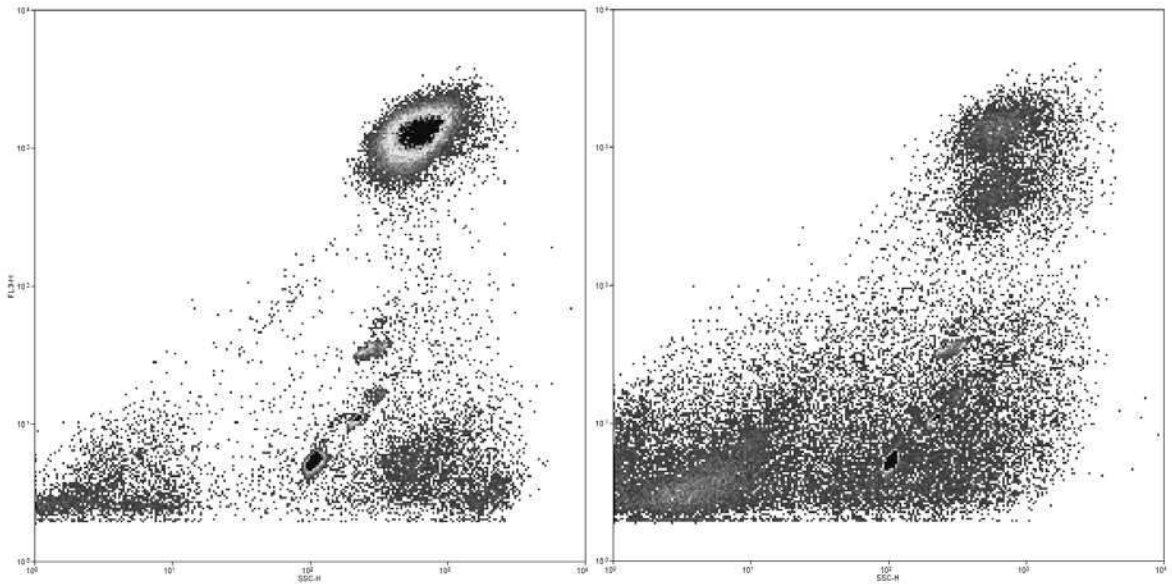806 standard deviation (n = 3). At day 18 and day 30, n = 1.

807

808   Figure 1

809
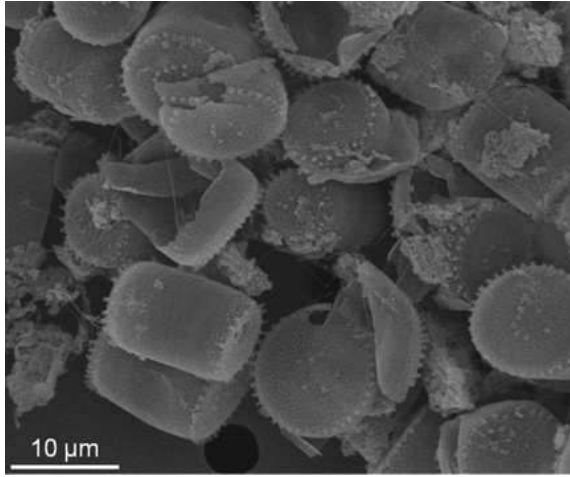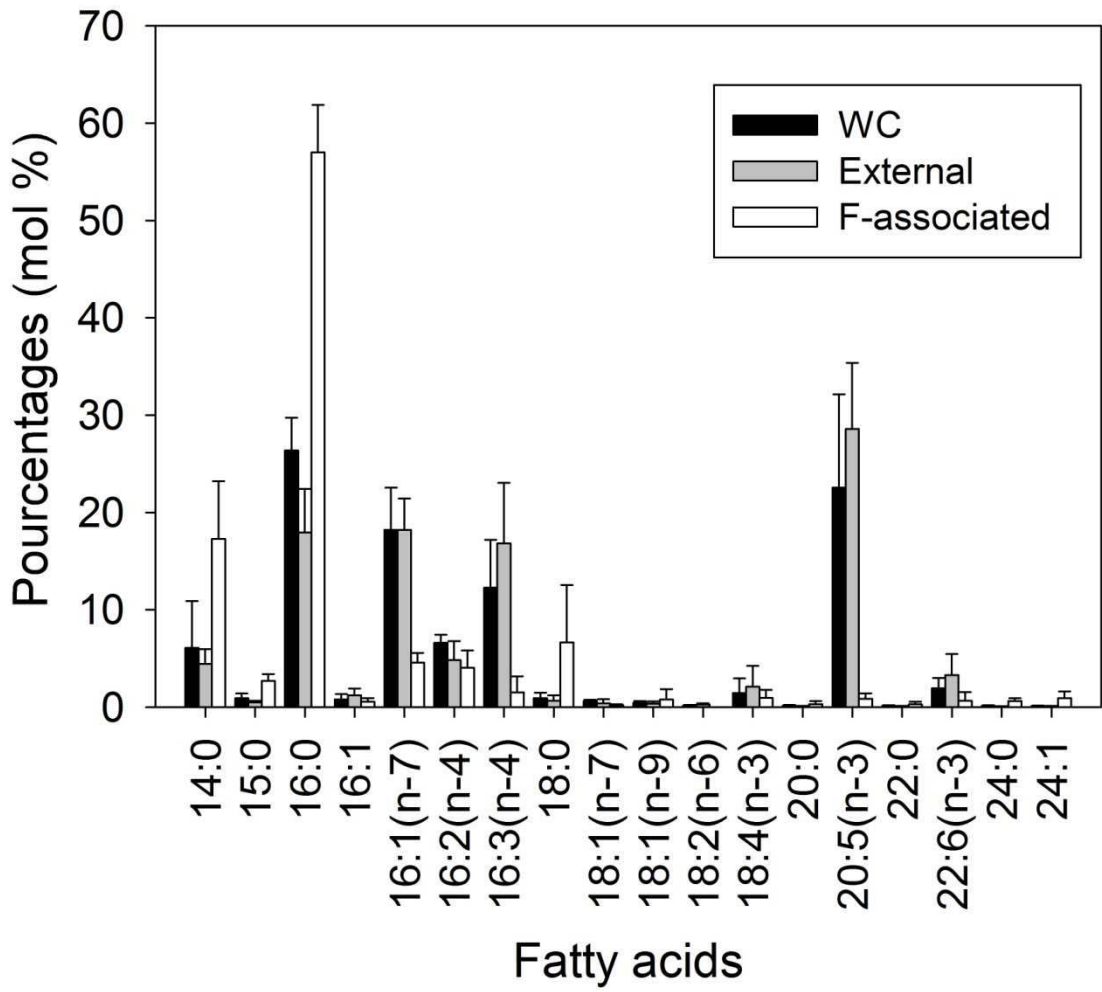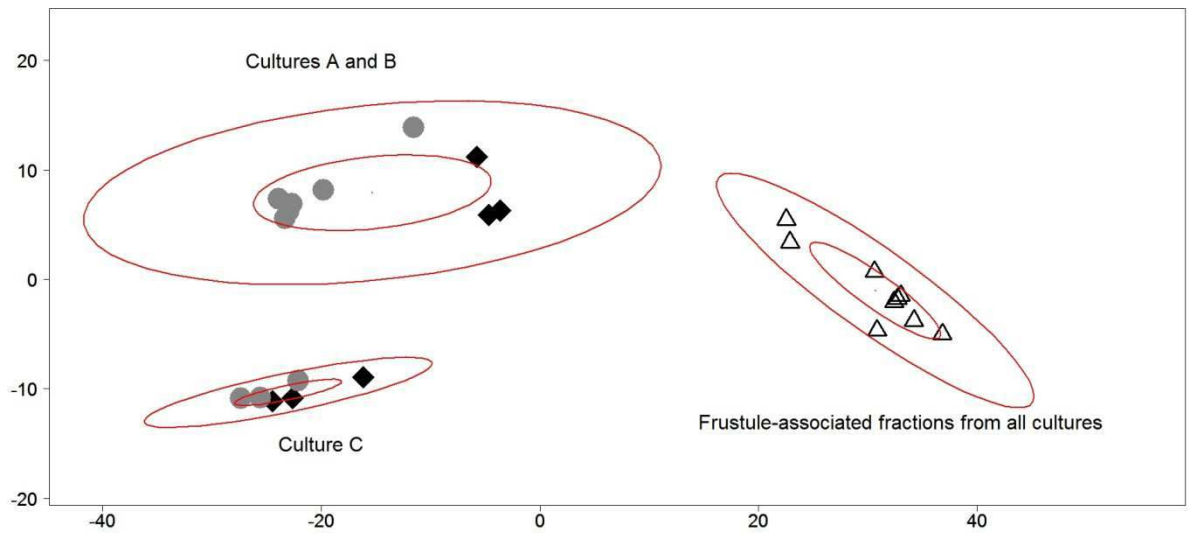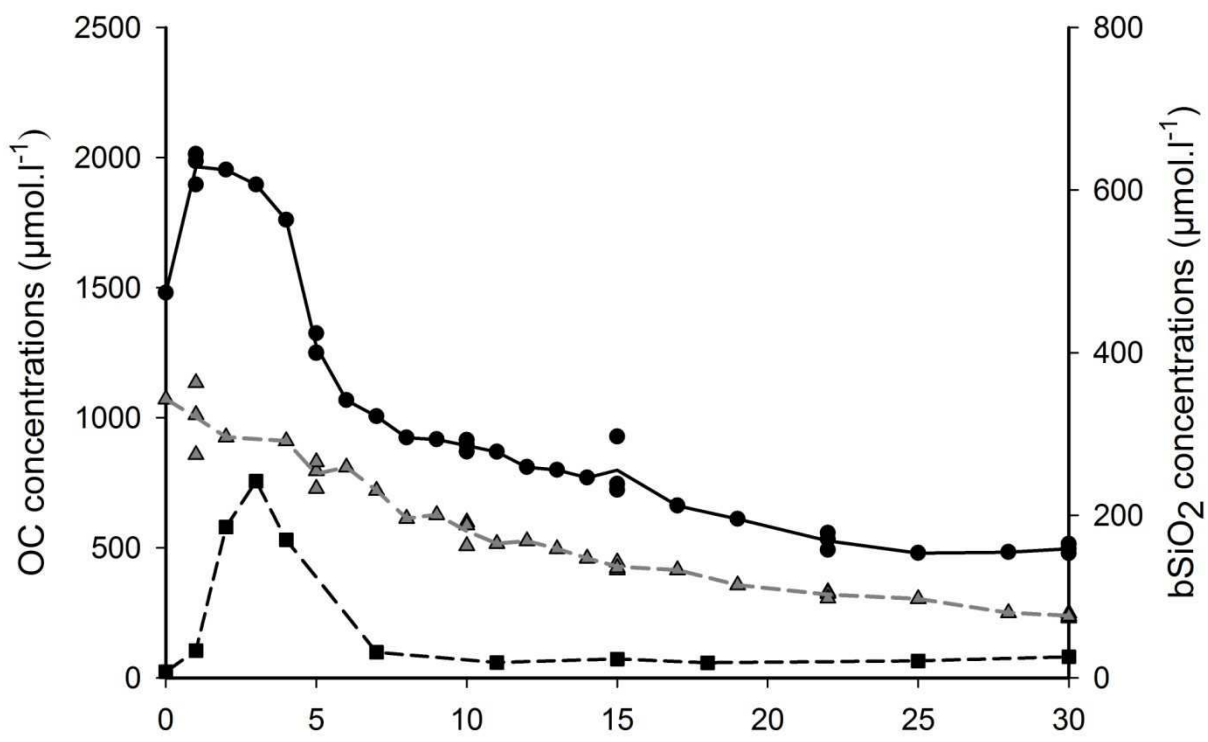

810

811

812

813   Figure 2.

814

815   Figure 3.

816

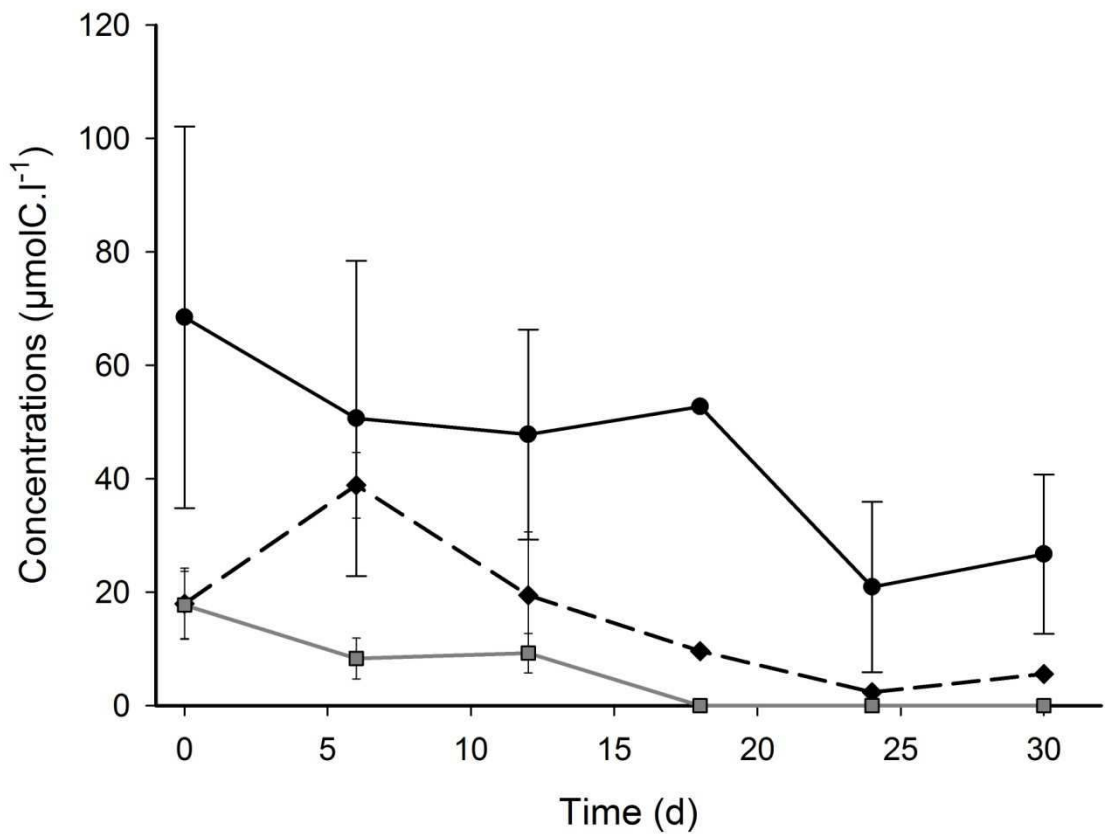817   Figure 4.

36

Cultures A and B

Culture C

Frustule-associated fractions from all cultures

818

819   Figure 5.

820

821   Figure 6.

822

Figure 7.

823

824
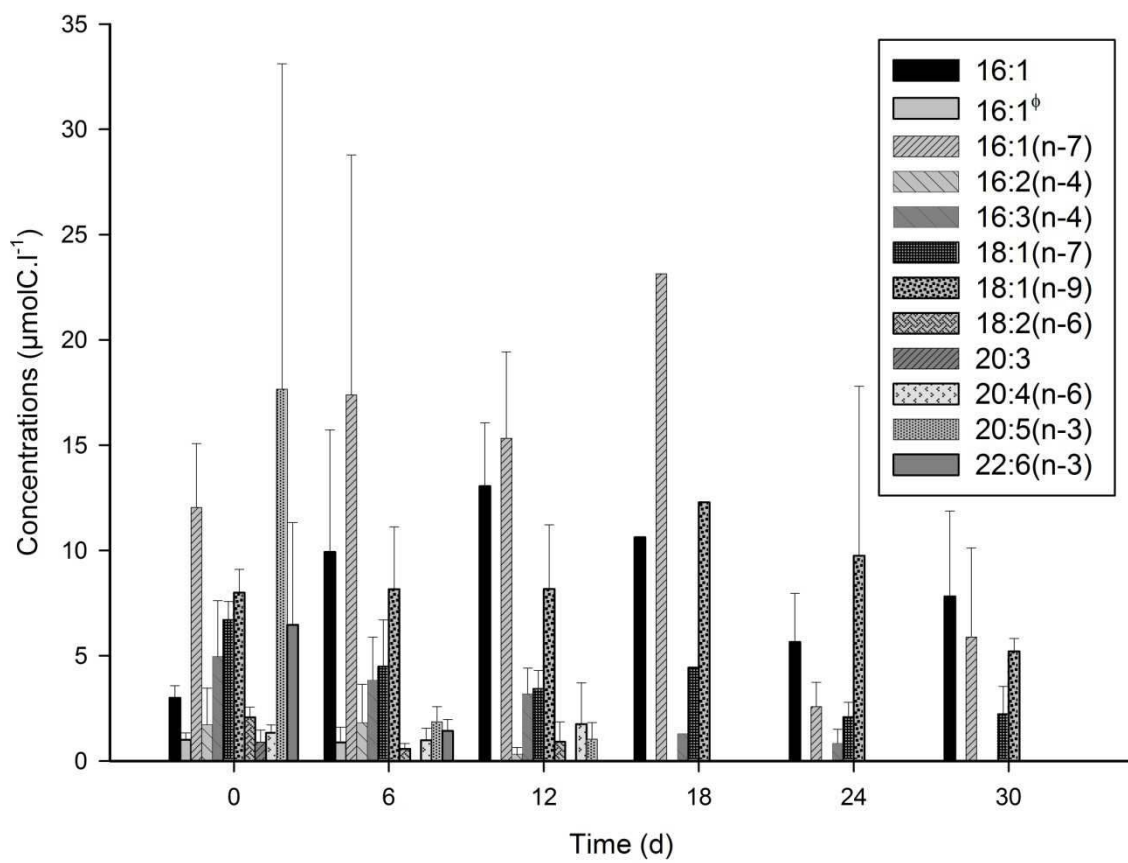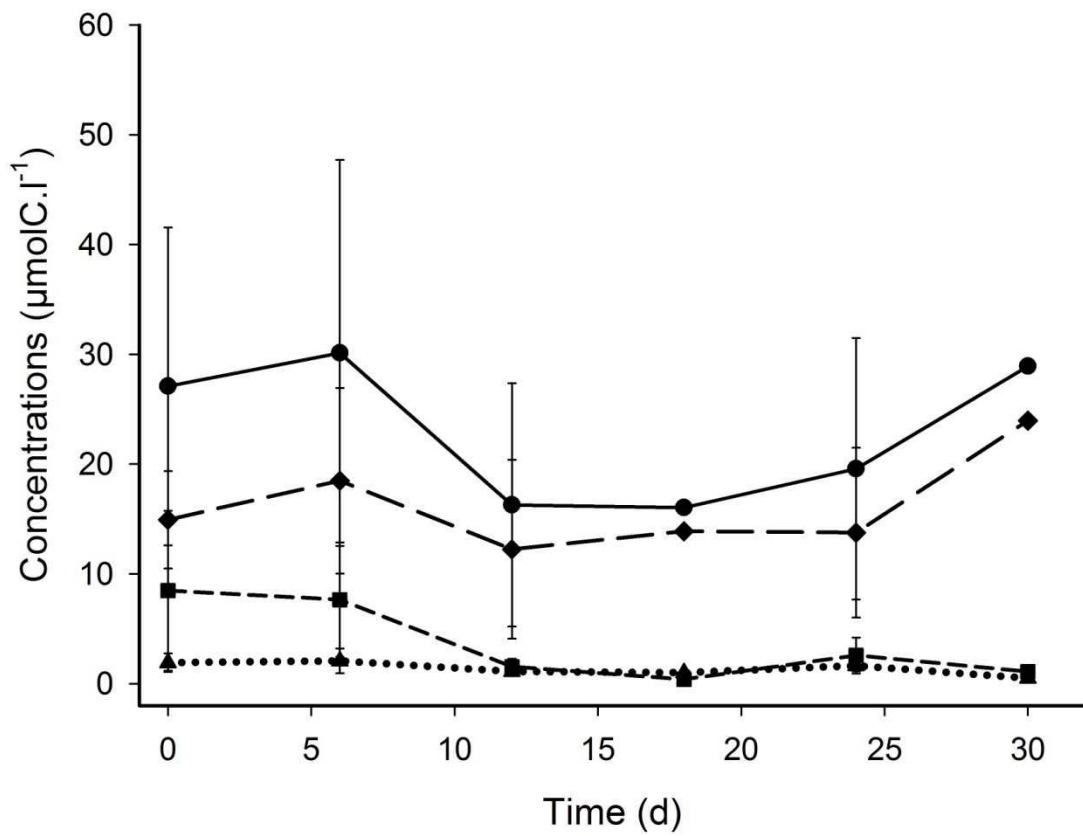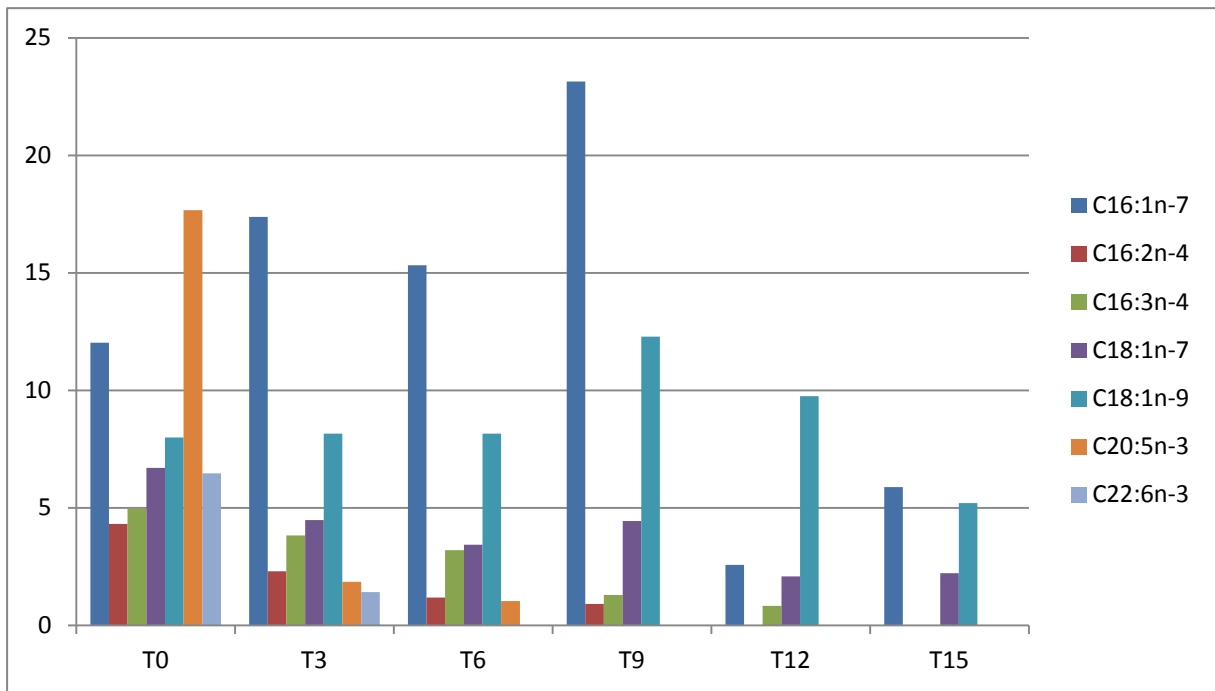
825

826   Figure 8.

827

828

829   Figure 9.

830

41